PCCP

Accepted Manuscript

ROYAL SOCIETY OF CHEMISTRY

www.rsc.org/pccp

Cite this: DOI: 10.1039/c0xx00000x

www.rsc.org/xxxxxx

ARTICLE TYPE

Thermoresponsive Fluorescence of Graphene-Polymer Composite Based on Local Surface Plasmons Resonance Effect

Yunyun Huang, Wensheng Lin, Kan Chen, Wenkai Zhang, Xudong Chen, * Ming Qiu Zhang,*

Received (in XXX, XXX) Xth XXXXXXXXX 20XX, Accepted Xth XXXXXXXXX 20XX

DOI: 10.1039/b000000x

ABSTRACT: A water-processable blue fluorescent silver nanoparticles@graphene-polymer composite (Ag@G-pNIPAM) consisting of graphene coated with a thermally responsive poly-(N-isopropylacrylamide) (pNIPAM) shell is prepared. The pNIPAM shell swells or collapses as a function of temperature, serving as a means to trap silver nanoparticles in solution and get them sufficiently close to the graphene core for providing fluorescence enhancement based on the local surface plasmons resonance (LSPR) effect. The unique thermoresponsive properties and high enhancement ratio of the material should find application in solution fluorescence enhancers and a variety of biomedical applications, such as cellular uptake, sensor and imaging.

1 Introduction

Fluorescent organic compounds play important roles in the development of low-cost optoelectronic devices.[1, 2] Due to the relatively expensive vacuum evaporation system required for making thin film of low-molecular-weight fluorescent organic compounds via deposition, [2] solution-processable fluorescence materials are obviously more attractive.

In the meantime, graphene has shown exciting prospects in both basic research and applications.[3] Although as a zero-bandgap semiconductor, fluorescence realization in visible wavelength stays a challenge hard to overcome,[4] controlling sp^2 clusters in sp^3 network by appropriate modification of graphene offers it the possibility of luminescence.[5] Fluorescence of graphene oxide (GO) ranges from visible (vis) to near-infrared wavelength (NIR), which favors its usage in fluorescence devices, biological sensors and fluorescent tags.[6,7] Nevertheless, the weak intensity of GO fluorescence is a huge obstacle.[8] Enhancement of graphene fluorescence in controllable way becomes a critical issue as a result. The interactions of fluorophores with metallic particles and surfaces (metals) have been used to obtain increased fluorescence intensities.[9] These years, new applications of novel metal nanoparticles go far beyond merely reflecting light and more attention have been paid on the interactions between metals and light in a field known as plasmonics.[10] Arrays of sub-wavelength holes in gold films were used as a substrate for enhanced fluorescence by surface plasmons.[11] Aslan and his co-workers enhance the fluorescence of Rhodamine 800 by plasmon effect of silver nanoparticles within several nanometer-distance.[12,13] And comparing with other novel metals, silver with many advantages is probably the most important material in plasmonics.[10] It is also well known that the local field effect responsible for the enhancement is distance dependent and maximizes in the surface.[11] Li and his co-workers have done a lot of work in designing hybrid nanoparticles combining the thermoresponsive property of poly-(N-isopropylacrylamide) (pNIPAM) and the metal-enhanced fluorescence (MEF) effect of Ag colloids to enhance the fluorescence of surface fluorophores.[14, 15] And these hybrid materials have shown brilliant potential application in many research fields.

Herein we develop a water-processable UV-blue fluorescent silver nanoparticles@graphene-polymer composite, consisting of graphene coated with thermally responsive pNIPAM shell (denoted by G-PNIPAM). The graphene cores provide the necessary fluorescence property, while pNIPAM shells swell or collapse in solution as a function of temperature, serving as a means to trap silver nanoparticles and get them sufficiently close to the graphene cores for generating fluorescence enhancement based on local surface plasmons resonance (LSPR) effect.

At present, there are a variety of methods of preparing inorganic nanoparticles-microgel hybrids, including well-defined core-shell structure[16-19] and well-dispersed nanoparticles in polymer micro-networks.[16,20,21] We choose pNIPAM as the shell substance because it possesses lower critical solution temperature (LCST) in water at ~32 °C,[22] near human body temperature, and is sensitive to pH value, concentration and chemical environment.[23] When pNIPAM is coupled with graphene, its LCST is raised to 38-39 °C (slightly higher than human body temperature) due to the restraint of the latter. If fluorescence of graphene can be enhanced by local surface plasmon resonance effect in terms of the temperature dependent habit of pNIPAM, the composite might be able to highlight abnormal temperature points in human body such as tumor.

2 Materials and methods

All the reagents were supplied by Aladdin and used without further purification. The graphene oxide (GO) in our work was

prepared by oxidizing graphite using a modified Hummer's method.[24]

2.1 Synthesis of G-pNIPAM composite

In order to attach pNIPAM, carboxylic groups were introduced to GO. This is done by taking graphene oxide in water (~4 mg/ml) and bath-sonicating it for 30 min. 4.8 g NaOH and 4 g chloroactic acid ($ClCH_2COOH$) by stirring and then sonicated the solution for 3 h. Carboxylic acid modified graphene oxide (G-COOH) was obtained after filtering and rinsing the solution. The product was purified and dried in vacuum.

PNIPAM-amine (NH_2-pNIPAM) was prepared by adding $NH_2CH_2CH_2SH$• HCl and azodiisobutyronitrile (AIBN) in methanol followed by 5 g NIPAM with nitrogen protection and then stirring for 20 h in 60 °C. The product was separated by ether and purified. Then it was dried in vaccum.

The G-COOH was diluted by water until it was $1*10^{-3}$ g/mL. 10 ml of this dispersion was added to 100 ml of NH_2-pNIPAM solution ($3*10^{-3}$ g/mL). Following, 0.06 g of N-3-dimethylaminopropy1-N'-ethylcarbodiimide hydrochloride (EDC) and 0.03 g of N-hydroxysuccinimide (NHS) were added and pH of the solution was adjusted by hydrochloric acid to 4.5. Then the solution was stirred for 48 h in 25 °C. The product went through dialysis, centrifuge and drying and then pNIPAMylated nano-graphene composite (G-pNIPAM) was obtained. Figure S1 presents the fabrication of G-pNIPAM by pNIPAM-amine and G-COOH.

2.2 Preparation of silver nanoparticles

0.169 g silver nitrate is dissolved in 100 mL ethanol with sonicationg bath for 30 min. The mixture was illuminated by UV irradiation (high pressure mercury lamp, 500 W, (365±10) nm) for 20 min. The products were washed with deionized water and ethanol for several times, and dried.

2.3 Preparation of Ag@G-pNIPAM composite system

An amount of silver nanoparticles/ethanol solution was added into G-pNIPAM solution until the solution comprising $6*10^{-5}$ g/L of G-pNIPAM and $4*10^{-5}$ M of Ag in 55 °C. This composite system was denoted as Ag@G-pNIPAM-55-1. In this system, pNIPAM chains collapsed and coated on the surface of graphene. Therefore, Ag nanoparticles were separated away from graphene. Then the system was cooled to 20 °C and denoted as Ag@G-pNIPAM-20-1. In this system, pNIPAM chains swelled. Following, the system was heated to 55 °C again and denoted as Ag@G-pNIPAM-55-2, in which Ag nanoparticles get close to graphene surface by pulling of pNIPAM chains, then to 20 °C and denoted as Ag@G-pNIPAM-20-2, in which Ag nanoparticles get far away from graphene by pushing of pNIPAM.

2.4 Preparation of large size silver particles

A mixture of 0.025 M silver nitrate, 5 M polyvinylpyrrolidone (PVP) and 0.125 M urotropine were stirred in 80 °C for 3 h. The products were washed with deionized water and ethanol for several times, and dried.

2.5 Characterization

Surface morphology and inner structure of Ag nanoparticles, G-pNIPAM and Ag@G-pNIPAM composites were observed by field emission scanning electron microscope (JSM-6330F and Hitachi S-4800, Japan), transmission electron microscope (JEM-2010HR, Japan) and atomic forece microscope (SPM-9500J3, Japan). The chemical compositions of the as-prepared films were investigated using Fourier transform infrared (FTIR) spectra (Nexus670 FTIR, America). The water contact angle were measured with a Krüss DSA 100 (Krüss Company, Ltd., Germany) apparatus at ambient temperature. The fluorescence spectra of the Ag@G-pNIPAM solution system were recorded using a RF-5301PC spectrofluorophotometer and the absorption spectra were collected using a UV-3150 UV-Vis-NIR spectrophotometer. Raman spectra were collected by a Renishaw inVia Raman system with 514.5 nm excitation.

3 Results and discussion

Details of preparation of G-pNIPAM are available in Electronic Supplementary Information (SI). Figure S1 presents the fabrication of G-pNIPAM by pNIPAM-amine (NH_2-pNIPAM) and carboxylic acid modified graphene oxide (G-COOH). Figures S1-S3 prove the formation of G-pNIPAM.[25, 26] Figure S4 indicates that the initial stage of phase separation of the polymer chains is perceived at a temperature slightly higher than 37 °C, while the LCST of pNIPAM on graphene is 39 °C.[27-31] It has been reported that in an acidic media, pNIPAM shows a better thermo-sensitivity and it will reduce the phase transition temperature of several degrees.[32] In order to get close to human body temperature, the fluorescence system in this work is operated in neutral media. Accordingly, two temperature points (20 and 55 °C) at different sides of 39 °C were selected for the subsequent study.

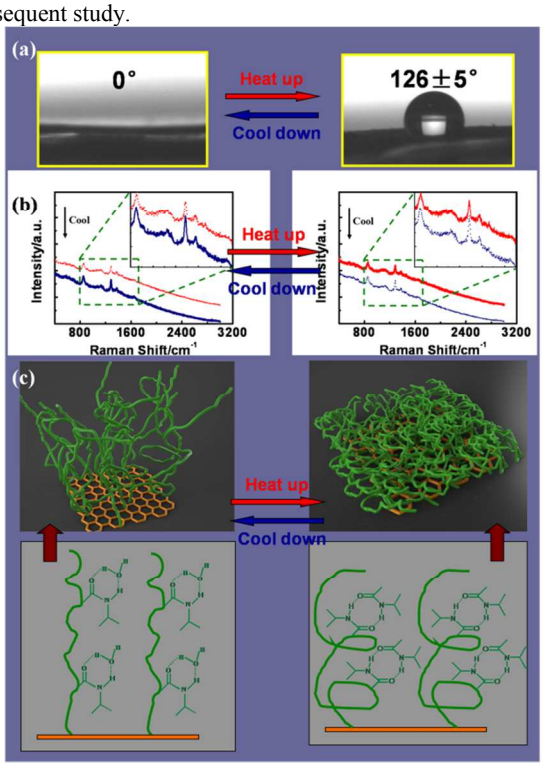

Figure 1. Thermally responsive wettability for a flat G-PNIPAM surface. (a) Change of water drop profile when temperature was elevated from 20 °C (left) to 55 °C (right) with water contact angles(CAs) of 0°and 126±5°, respectively. (b) Raman spectra and (c) Diagram of reversible formation of intermolecular hydrogen bonding between PNIPAM chains and water molecules (left) and intramolecular hydrogen bonding between C=O and N-H groups in PNIPAM chains (right) below and above the LCST, which is considered to be the molecular mechanism of the thermally responsive wettability of a G-PNIPAM thin film.

Figure 1 depicts thermally responsive wettability and Raman spectra of a flat G-pNIPAM surface collected at 20 and 55 °C, respectively. Switching of surface wetting and the corresponding Raman shift originate from reversible formation of (i) intermolecular hydrogen bonding between pNIPAM chains and water molecules and (ii) intramolecular hydrogen bonding between C=O and N-H groups in pNIPAM chains below and above the LCST.[33, 34] Establishment and deconstruction of the two interactions are believed to be the molecular mechanism involved, [35] which is further confirmed by Figure S5.

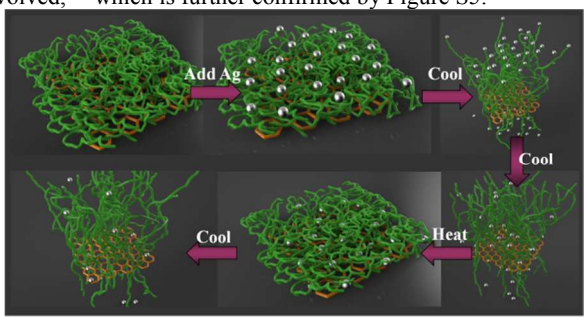

Figure 2. Schematic model showing the controllable plasmon process of silver nanoparticles to graphene in the cooling-heating-cooling cycle.

Figure 2 shows the controllable distance between silver nanoparticles and graphene cores at different temperatures. At 55 °C that is higher than LCST, pNIPAM chains on graphene contract and wrap graphene to a state of tightly packed globular particles. When a certain amount of silver dispersion is added, the nanoparticles have to be isolated from the graphene cores by the packed pNIPAM layer. With decreasing temperature to 20 °C, the pNIPAM chains are gradually swelled. Ag nanoparticles should quickly spread over the polymer network as driven by the concentration gradient, but it takes quite a while to complete the job in reality because of the size effect of the particles (~40 nm). Consequently, the nanoparticles are firstly pushed away by the swollen polymer, and then diffuse into the interstitial sites of stretched macromolecular chains.[36] When the solution is heated from 20 °C to LCST, polymer chains on graphene are extended becoming well-solvated random coils and hence more silver nanoparticles are included. In the case of higher temperature (*i.e.* > LCST), pNIPAM shrinks, bringing the silver nanoparticles to graphene surface. When temperature reaches 55 °C, the collapsed polymer microgel wraps the Ag nanoparticles on the graphene surface. As for the second cooling down to below LCST (55 → 20 °C), the polymer chains spread out again, and the silver nanoparticles travel to the solution away from graphene surface. When temperature is higher than LCST once more, the swollen pNIPAM chains are dehydrated and shrunk, and give rise to final collapsed volumes of less than 50 % the swollen microgel volume.[37] For the reason that Ag nanoparticles remain in the Ag@G-pNIPAM composite system throughout the whole process and above processes are completely reversible,[38] and thus promise the reversible control of distance between fluorescent graphene and Ag nanoparticles. Álvarez-Puebla and the co-workers[39] realized the distance control between 1-naphthalenethiol and Au core, which presented a similar approach like ours.

The relative positions of Ag nanoparticles and G-pNIPAM at different temperatures are shown in Figure 3. Having been grafted by pNIPAM, graphene becomes thicker (SEM, Figure 3a1, b1 and c1) and the surface electron diffraction patterns and lattice[40] become fuzzy (TEM, Figure 3a2, b2 and c2). It proves that pNIPAM has been bonded to graphene from another angle. Moreover, AFM images (Figure 3a3, b3 and c3) indicate that the G-pNIPAM composite seems to be an ellipsoid tightly wrapped by pNIPAM with diameter of ~300 nm and height of ~40 nm. Only polymer phase[41] can be seen in the phase trace.

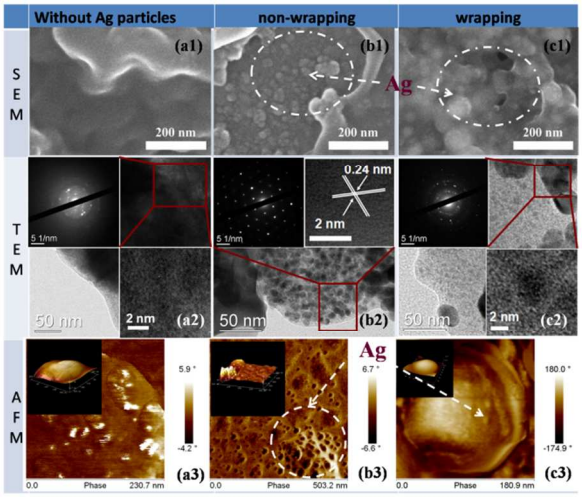

Figure 3. SEM (a1, b1, c1), TEM (a2, b2, c2) images and phase images of AFM (a3, b3, c3) of G-PNIPAM without Ag nanoparticles (a), Ag@G-PNIPAM non interacting with Ag nanoparticles (b) and Ag@G-PNIPAM interacting with small Ag nanoparticles (c).Selected area electron diffraction (SAED) patterns are given in (a2), (b2) and (c2). And height images of AFM are given in (a3), (b3) and (c3).

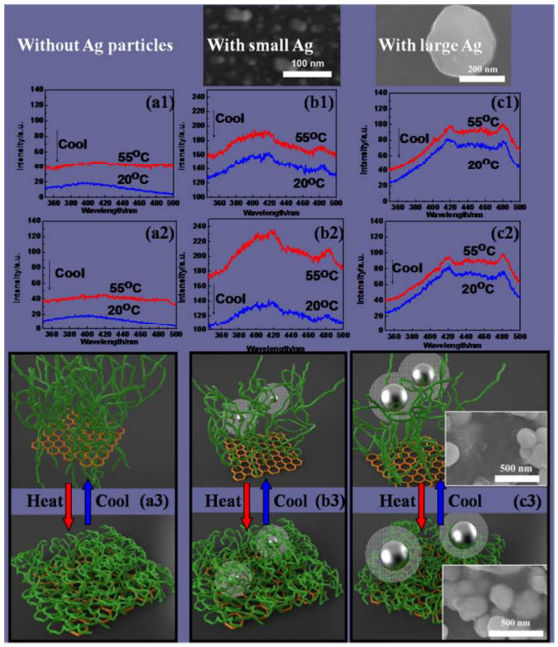

Figure 4. Fluorescence spectra （FL）(a1, a2, b1, b2, c1 and c2) and schematic (a3, b3, c3) of the G-PNIPAM without Ag particles (a), G-PNIPAM with small Ag nanoparticles (b) and G-PNIPAM with large Ag nanoparticles (c) in cooling-heating-cooling cycle. Insets of (c3) are SEM images of the large Ag nanoparticles added in the G-PNIPAM solution

system and never diffuse through the porous polymer shell at 20 and 55 °C, respectively.

In Figure 3b, the collapsed polymer tightly wraps the graphene, hindering diffusion of Ag nanoparticles and the graphene core cannot be reached (which is corresponding to the 2nd image first line in Figure 2). There are Ag nanoparticles with a diameter of ~40 nm on the composite surface (SEM, Figure 3b1). Clear electron diffraction patterns of Ag crystals showing lattice space of 0.24 nm[42] are recorded (TEM, Figure 3b2). In AFM image of Figure 3b3, two phases with different hardness are observed as a result of harder Ag nanoparticles standing on the softer polymer surface. In contrast, Figure 3c3 exhibits that Ag nanoparticles have diffused into the polymer network and only the collapsed polymer is visible (which is corresponding to the 2nd image second line in Figure 2). This analysis is proved by SEM image of Ag nanoparticles covered by a polymer layer (Figure 3c1), blurring SEAD and lattice (Figure 3c2), and a smooth ellipsoid with diameter of ~300 nm and height of ~100 nm (larger than ~40 nm of G-pNIPAM) (Figure 3c3). In this context, the structure characterization has confirmed the movement mechanism of polymer and Ag nanoparticles speculated in Figure 2.

Ag nanoparticles are employed to enhance fluorescence of the composite system because they could produce localized surface plasmon resonances (LSPR) when exposed to light with certain wavelength.[37] Surface-enhanced fluorescence (SEF) occurs primarily as a result of the interactions between the excited state of a fluorophore with the near-fields of an excited metal nanostructure. The distance dependence of fluorescence for emitters within the metal structure has been demonstrated by several authors in a variety of system[38, 39] and is consistently found to reach a maximum for fluorophores located within ~10 nm from the metallic surface.[18] Fluorescence (FL) spectra and schematic of the G-PNIPAM without Ag particles, G-PNIPAM with small Ag nanoparticles and large Ag nanoparticles in repeated cooling-heating cycles are shown in Figure 4. Fluorescence of the composite system without Ag nanoparticles is rather weak, which is marginally intensified at high temperature due to aggregation enhancement.[46]

When Ag nanoparticles are added to the solution of collapsed microgel (55 °C), the collapsed polymer hinders the diffusion of Ag nanoparticles and graphene core cannot be reached. Hence no obvious SEF signal is detected (Figure 4b1). Cooling the system to 20 °C, micropores appear in the swollen polymer network. However, because the Ag nanoparticles with 40 nm-diameter can not diffuse into the network quickly enough, the swollen polymer pushes Ag nanoparticles away from graphene surface and the fluorescence is similar to that with Ag nanoparticles. In the process of heating again from 20 °C to 55 °C, pNIPAM chains stretch when temperature increases below 39 °C. Ag nanoparticles can easily diffuse through the polymer network by the force of concentration difference. Above 39 °C, polymer chains collapses again, and Ag nanoparticles diffusing in the polymer network are pulled to the graphene surface by the collapsed polymer so that graphene is close enough with Ag nanoparticles to react with the silver LSPR effect, which effectively enhances graphene fluorescence of an enhancement ratio of 1.7 (see Supplementary Information for details about enhancement ratio calculation)[47] (Figure 4b2). Cooling again, the Ag nanoparticles on graphene surface are pushed away by swollen polymer again. Graphene and Ag nanoparticles are too far to interact by LSPR effect (Figure 4c2). Fluorescence intensity decreases again (Figure 4b2). Moreover, reversible fluorescence enhancement induced by LSPR effect of Ag nanoparticles is obtained in cooling-heating cycle as above. UV-vis absorption spectra consistent with fluorescence enhancement effect are shown in Figure S6. Therefore, it can be included that LSPR effect of Ag nanoparticles enhances the graphene fluorescence by increasing its absorption efficiency[45] when temperature is above the polymer's LCST.[39] For the reason that Ag nanoparticles remain in the system in the whole process, the system possesses reversibility. And the distance dependence of fluorescence for emitters within the local resonant SP-field has been found to reach a maximum for fluorophores located within ~10 nm from the metallic surface,[18] so when separated by pNIPAM, free Ag nanoparticles have no influence on the system fluorescence.

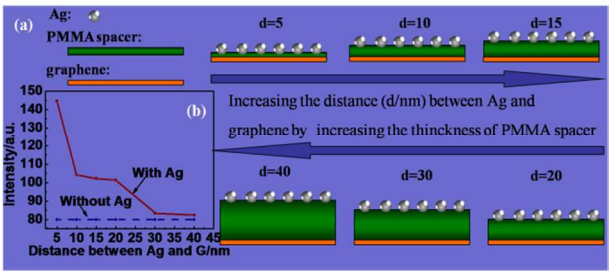

Figure 5 Control experiment of fluorescence intensity depending on the distance between Ag particles and graphene (G). (a) Control experiment model realizing different distances between Ag particles and G; (b) Fluorescence intensity depending on the distance between Ag particles and G.

To confirm the mechanism of graphene/Ag nanoparticles distance control by the thermal-responsive polymer, control experiments employing Ag nanoparticles with different sizes are conducted. In Figure 4c, Ag nanoparticles with diameter >200 nm are added to the composite system and no obvious fluorescence enhancement is detected during the same cooling-heating cycle as that in Figure 4b. Also, no obvious absorption enhancement can be observed in Figure S6c. SEM images in Figure 4c3 reveal that Ag nanoparticles stay on the polymer surface all the time and never reach to graphene either when added to the collapsed microgel (55 °C) or when the polymer undergoes swollen process. The Ag nanoparticles are too large to diffuse through the polymer network. It confirms that nanoparticles with sizes larger than a certain limit could not easily diffuse through the polymer network so resultantly the graphene fluorescence could not be enhanced,[48, 49] which confirms the control mechanism above.

Meanwhile, a control experiment is done by measuring fluorescence intensity as a function of distance between Ag nanoparticles and graphene (Figure 5). Firstly, graphene, PMMA layer and Ag nanoparticles layer were successively spun on quartz surface. The distance between graphene and Ag nanoparticles varies from 0 to 40 nm by adjusting the thickness of PMMA layer (Figure 5a). Clearly, fluorescence intensity decreases with the increase of distance between Ag nanoparticles and graphene (Figure 5b), confirming the mechanism discussed

above.

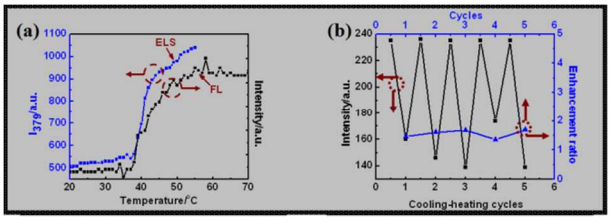

Figure 6 (a) Fluorescence (FL) intensity depending on temperatures of Ag@G-pNIPAM and (b) Reversibility of controllable fluorescence intensity in more than 5 cooling-heating cycles.

Since the distance of Ag nanoparticles and graphene is controlled by the thermal-sensitivity of pNIPAM, the significant fluorescence enhancement occurs when temperature is higher than 38 °C (red line in Figure 6a), which agrees with the LCST of G-pNIPAM (blue line in Figure 6a). It is the reversible collapse and swelling of pNIPAM, which realize the reversibility of controllable fluorescence enhancement (Figure 6b). Considering the number of Ag nanopartles diffusing through the polymer network to graphene surface in every cooling-heating cycle can not stay the same, the enhancement ratio in every cycle also may not be accurately the same. However, it stays between 1.4-2.0, which can be seen in Figure 6b.

Furthermore, absorption spectra in Figure S7 reveal that not only can this thermal-responsive system be applied in LSPR enhancing fluorescence, but also in establishing new fluorescence devices by fluorescent probe. This result confirms the graphene-Ag nanoparticles-distance control mechanism by thermal-responsive polymer on the other side. That is, the polymer chains grafted on graphene surface pull Ag nanoparticles to graphene surface at a temperature above its LCST, inducing graphene in the LSPR field of Ag nanoparticles, while pushing them away from graphene surface and inducing the graphene out of their LSPR field in case of temperature below its LCST.

Conclusions

From the discussion above, a solution-processible optical platform that can realize thermal-responsive fluorescence enhancement by polymer thermal-sensitivity based on LSPR effect of Ag nanoparticles is established. The unique thermoresponsive property and high enhancement ratio should find applications in solution fluorescence enhancers[50] and a variety of biomedical applications,[51] such as cellular uptake[52] and imaging.[53]

Notes and references

Key Lab Polym Compos & Funct Mat, Key Lab Designed Synth & Appl Polym Mat, School of Chemistry and Chemical Engineering, Sun Yat-sen University, Guangzhou, 510275 (China). E-mail: cescxd@mail.sysu.edu.cn (X.D. Chen); ceszmq@mail.sysu.edu.cn (M. Q. Zhang)

† Electronic Supplementary Information (ESI) available: Experimental details, structure analysis of the as-prepared materials and UV absorption spectra of the as-prepared systems are available in Supporting Information. See DOI: 10.1039/b000000x/

Acknowledgments

We thank the financial support from the Natural Science Foundations of China (Grant No. 51233008 and 51173215).

Reference

1 J. R .Sheats, H. Antoniadis, M. Hueschen, W. Leonard, J. Miller, R. Moon, D. Roitman, and A.vStocking, *Science,* 1996, **273**, 884-888.
2 L. J. Rothberg and A. J. Lovinger, *J. Mater. Res*., 1996, **11,** 3174-3187.
3 A. K. Geim, K. S. Novoselov, *Nat. Mater*., 2007, **6**, 183-191.
4 K. S. Novoselov, A. K. Geim, S. V. Morozov, D. Jiang, Y. Zhang, S. V. Dubonos, I. V. Grigorieva and A. A. Firsov, *Science,* 2004, **306**, 666-669.
5 G. Eda, Y. Lin, C. Mattevi, H. Yamaguchi, H. Chen, I. Chen, C. Chen and M. Chhowalla, *Adv. Mater*., 2010, **22,** 505-509.
6 X. Sun, Z. Liu, K. Welsher, J. T. Robinson, A. Goodwin, S. Zaric, H. Dai, *Nano Res*., 2008, **1**, 203-212.
7 Z. Liu, J. T. Robinson, X. Sun, H. Dai, *J. Am. Chem. Soc*., 2008, **130**, 10876-10877.
8 R. Contreras-Cáceres, J. Pacifico, I. Pastoriza-Santos, J. Pérez-Juste, A. Fernández-Barbero and L. M. Liz-Marzán, *Adv. Funct. Mater*., 2009, **19**, 3070-3076.
9 J. R. Lakowicz, *Anal. Biochem.*, 2005, **337**, 171-194.
10 M. Rycenga, C. M. Cobley, J. Zeng, W. Li, C. H. Moran, Q. Zhang, D. Qin, Y. Xia, *Chem. Rev.*, 2011, **111**, 3669-3712.
11 A. G. Brolo, S. C. Kwok, M. G. Moffitt, R. Gordon, J. Riordon, K. L. Kavanagh, *J. Am. Chem. Soc.*, 2005, **127**, 14936-14941.
12 K. Aslan, M. Wu, J. R. Lakowicz, C. D. Geddes, *J. Fluoresc.,* 2007, **17**, 127-131.
13 K. Aslan, M. Wu, R. Joseph, J. R. Lakowicz, C. D. Geddes, *J. Am. Chem. Soc.,* 2007, **129**, 1524-1525.
14 F. Tang, N. Ma, X. Wang, F. He, L. Li, *J. Mater. Chem.*, 2011, **21**, 16943-16948.
15 L. Tong, N. Ma, F. Tang, D. Qiu, Q. Cui, L. Li, *J. Mater. Chem.*, 2012, **22**, 8988-8993.
16 M. Karg, I. Pastoriza-Santos, L. M. Liz-Marzán, T. A. Hellweg, *ChemPhysChem,* 2006, **7**, 2298-2301.
17 Y. Lu, Y. Mei, M. Drechsler and M. Ballauff, *Angew. Chem. Int. Ed*., 2006, **45**, 813-816.
18 D. J. Kim, S. M. Kang, B. Kong, W. J. Kim, H. J. Paik and I. S. Choi, *Macromol. Chem. Phys*., 2005, **206**, 1941-1946.
19 D. Suzuki and H. Kawaguchi, *Langmuir,* 2006, **22**, 3818-3822.
20 Y. Lu, Y. Mei, M. Ballauff and M. Drechsler, *J. Phys. Chem. B,* 2006, **110**, 3930-3937.
21 M. Karg, I. Pastoriza-Santos, J. Pérez-Juste, T. Hellweg and L. M. Liz-Marzán, *Small,* 2007, **3**, 1222-1229.
22 E. S. Gil and S. M. Hudson, *Prog. Polym. Sci*. 2004, **29**, 1173-1222.
23 S. Nayak and L. A. Lyon, *Angew. Chem. Int. Ed*. 2005, **44**, 7686-7708.
24 T. Ramanathan, A. A. Abdala, S. Stankovich, D. A. Dikin, M. Herrere-Alonso, R. D. Pinger, D. H. Adamson, H. C. Schniepp, X. Chen, R. S. Ruoff, S. T. Nguyen, I. A. Aksay, R. K. Prud'homme and L. C. Crinso, *Nat. Nanotechnol*., 2008, **3**, 327-331.
25 C. Hong, Y. You and Pan, C. *Chem. Mater*., 2005, **17**, 2247-2254.
26 Chen, G. And A. S.Hoffman, *Nature,* 1995, **373**, 49-52.
27 T. G. Park and A. S. Hoffman, *J. Appl Polym. Sci*., 1994, **52**, 85-89.
28 D. H. Xie, X. D. Ye, Y. W. Ding, G. Z. Zhang, N. Zhao, K. Wu, Y. Cao and X. X. Zhu, *Macromolecules*, 2009, **42**, 2715-2720.
29 Y. L. Guo, B. J. Sun and P. Y. Wu, *Langmuir*, 2008, **24**, 5521-5526.
30 W. Lu, B. S. Fernández Band, Y. Yu, Q. G. Li, J. C. Shang, C. Wang, Y. Fang, R. Tian, L. P. Zhou, L. L. Sun, Y. Tang, S. H. Jing, W. Huang and J. P. Zhang, *Acta* 2007, **158**, 29-58.
31 Y.Xia, A. D. Burke and H. D. H. StÖver, *Macromolecules*, 2006, **39**, 2275-2283.
32 M. Karg, I. Pastoriza-Santos, B. Rodriguez-González, R. Klitzing, S. Wellert, T. Hellweg, *Langmuir*, 2008, **24**, 6300-6306.
33 J. Dybal, M. Trchová, P. Schmidt Vib. *Spectrosc*., 2009, **51**, 44-51.
34 Z. Ahmed, E. A. Gooding, K. V. Pimenov, L. Wang and S. A. Asher, *J. Phys. Chem. B,* 2009, **113**, 4248-4256.
35 T. Sun, G. Wang, L. Feng, B. Liu, Y. Ma, L. Jiang and D. Zhu, *Angew. Chem. Int. Ed*., 2004, **43**, 357-360.

36 R. A. Álvarez-Puebla, D. S. D. Santos and J. R. F. Aroca, *Analyst,* 2004, **129**, 1251-1256.
37 B. Sierra-Martin, Y. Choi, M. S. Romero-Cano, T. Cosgrove, B. Vincent and A. Fernandez-Barbero, *Macromolecules,* 2005, **38**, 10782-10787.
38 O. Kulakovich, N. Strekal, A. Yaroshevich, S. Maskevich, S. Gaponenko, I. Nabiev, U. Woggon, M. Artemyev, *Nano Lett.*, 2002, **2**, 1449-1452.
39 E. Dulkeith, M. Ringler, T. A. Klar, J. Feldmann, A. M. Javier, W. J. Parak, *Nano Lett.*, 2005, **5**, 585-589.
40 R. Contreras-Cáceres, A. Sánchez-Iglesias, M. Karg, I. Pastoriza-Santos, J. Pérez-Juste, J. Pacifico, T. Hellweg, A. Fernández-Barbero and L. M. Liz-Marzán, *Adv. Mater.*, 2008, **20**, 1666-1670.
41 R. A. Álvarez-Puebla, R. Contreras-Cáceres, I. Pastoriza-Santos, J. Pérez-Juste and L. M. Liz-Marzán, *Angew. Chem. Int. Ed.*, 2009, **48**, 138-143.
42 P. Y. Huang, C. S. Ruiz-Vargas, A. M. Zande, W. S. Whitney, Levendorf, M. P.; Kevek, J. W.; Garg, S.; Alden, J. S.; Hustedt, C. J.; Y. Zhu, J. Park, P. L. McEuen and D. A. Muller, *Nature,* 2011, **469**: 389-393.
43 Plunkett, K. N.; Zhu, X.; Moore, J. S.; Leckb and, D. E. *Langmuir* **2006**, *22*: 4259-4266.
44 I. Pastoriza-Santos and L. M. Liz-Marzán, *J. Mater. Chem*., 2008, **18**: 1724-1737.
45 C. Gao, Z. Lu, Y. Liu, Q. Zhang, M. Chi, Q. Cheng and Y. Yin, *Angew. Chem. Int. Ed*., 2012, **51**, 5629-5633.
46 Y. Hong, J. W. Y. Lam and B. Tang, *Chem. Soc. Rev*., 2011, **40**, 5361-5388.
47 M. Rycenga, C. M. Cobley, J. Zeng, W. Li, C. H. Moran, Q. Zhang, D. Qin and Y. Xia, *Chem. Rev*., 2011, **111**, 3669-3712.
48 R. G. Pearson, *J. AM. Chem. Soc*., 1963, **85**, 3533-3539.
49 R. G. Pearson, *Science,* 1966, **151**, 172-177.
50 K. Aslan, M. Wu, J. R. Lakowicz and C. D. Geddes, *J. Am. Chem. Soc.*, 2007, **129**, 1524-1525.
51 S. G. Penn, L. He and M. J. Natan, *Curr. Opin. Chem. Biol*., 2003, **7**, 609-615.
52 J. Kneipp, H. Kneipp, M. Mclaughlin, D. Brown and K. Kneipp, *Nano Lett*., 2006, **6**, 2225-2231.
53 X. M. Qian and S. M. Nie, *Chem. Soc. Rev.*, 2008, **37**, 912-920.

The pNIPAM shell traps silver nanoparticles in solution and get them close to the graphene core for providing fluorescence enhancement.

Yunyun Huang, Wensheng Lin, Kan Chen, Wenkai Zhang, Xudong Chen*, Ming Qiu Zhang*

Title: Thermoresponsive Fluorescence of Graphene-Polymer Composite Based on Local Surface Plasmons Resonance Effect